PL-TR-96-2311 MFD-96-TR-15649

NETWORK IDENTIFICATION PERFORMANCE: (1) SIMULATIONS FOR THE MIDDLE EAST/NORTH AFRICA, AND (2) MAXIMUM LIKELIHOOD ESTIMATES OF TELESEISMIC m_b FOR THE GSETT-3 PRIMARY NETWORK

T. G. Barker

Maxwell Technologies - Federal Division
8888 Balboa Avenue
San Diego, CA 92123-1506

September 1996

Scientific Report No. 1

DEPARTMENT OF ENERGY
OFFICE OF NONPROLIFERATION AND NATIONAL SECURITY
WASHINGTON, DC 20585

PHILLPS LABORATORY
Directorate of Geophysics
AIR FORCE MATERIEL COMMAND
HANSCOM AFB, MA 01731-3010

SPONSORED BY
Department of Energy
Office of Non-Proliferation and National Security

MONITORED BY
Phillips Laboratory
CONTRACT No. F19628-95-C-0111

The views and conclusions contained in this document are those of the authors and should not be interpreted as representing the official policies, either express or implied, of the Air Force or U.S. Government.

This technical report has been reviewed and is approved for publication.

Delaine Reiter
DELAINE R. REITER
Contract Manager
Earth Sciences Division

James F. Lewkowicz
JAMES F. LEWKOWICZ
Director
Earth Sciences Division

This report has been reviewed by the ESD Public Affairs Office (PA) and is releasable to the National Technical Information Service (NTIS).

Qualifed requestors may obtain copies from the Defense Technical Information Center. All others should apply to the National Technical Information Service.

If your address has changed, or you wish to be removed from the mailing list, or if the addressee is no longer employed by your organization, please notify PL/IM, 29 Randolph Road, Hanscom AFB, MA 01731-3010. This will assist us in maintaining a current mailing list.

Do not return copies of this report unless contractual obligations or notices on a specific document requires that it be returned.

REPORT DOCUMENTATION PAGE

Form Approved
OMB No. 0704-0188

1. AGENCY USE ONLY *(Leave blank)*

2. REPORT DATE
September 1996

3. REPORT TYPE AND DATES COVERED
Scientific Report No. 1

4. TITLE AND SUBTITLE
Network Identification Performance: (1) Simulations for the Middle East/North Africa and (2) Maximum Likelihood Estimates of Teleseismic m_b for the GSETT-3 Primary Network

5. FUNDING NUMBERS
Contract No.F19628-95-C-0111
PE 69120H
PR DENN TA GM
WU AC

6. AUTHOR(S)
Terrance G. Barker

7. PERFORMING ORGANIZATION NAME(S) AND ADDRESS(ES)
Maxwell Technologies - Federal Division
8888 Balboa Avenue
San Diego, CA 92123-1506

8. PERFORMING ORGANIZATION REPORT NUMBER
MFD-TR-96-15649

9. SPONSORING/MONITORING AGENCY NAME(S) AND ADDRESS(ES)
Phillips Laboratory
29 Randolph Road
Hanscom Air Force Base, MA 01731-3010
Contract Manager: Delaine Reiter/GPE

10. SPONSORING/MONITORING AGENCY REPORT NUMBER
PL-TR-96-2311

11. SUPPLEMENTARY NOTES
This research was sponsored by the Department of Energy, Office of Non-Proliferation and National Security, Washington, DC 20585

12a. DISTRIBUTION/AVAILABILITY STATEMENT
Approved for public release; distribution unlimited

12b. DISTRIBUTION CODE

13. ABSTRACT *(Maximum 200 words)*

We have simulated the detection and identification performance of the current and proposed IMS seismic networks in the Middle East/North Africa. The identification performance of a network is strongly dependent upon regional source and propagation variability. However, knowledge of those variations allow one to estimate their effects and to know that in some areas certain discriminants can work and in other areas they do not. Data sources included published results on wave propagation in this region and incorporated analyses of data taken by Vernon, *et al*, (1996) in Saudi Arabia.

The maximum likelihood estimates of magnitude (Ringdal, 1976) was developed to improve measures of signal amplitudes which are below detection levels in some or all of the network As pointed out by Von Seggern and Rivers (1978), values of m_b derived from arithmetic mean tend to have a positive bias, which may be eliminated by the use of maximum likelihood estimates. In this report, we simulate a suite of earthquakes recorded at the GSETT-3 Alpha network, and compare the m_b ís computed using the two methods with true values.

14. SUBJECT TERMS
seismology
seismic discrimination
Monte Carlo simulations
regional propagation

15. NUMBER OF PAGES
32

16. PRICE CODE

17. SECURITY CLASSIFICATION OF REPORT	18. SECURITY CLASSIFICATION OF THIS PAGE	19. SECURITY CLASSIFICATION OF ABSTRACT	20. LIMITATION OF ABSTRACT
Unclassified	Unclassified	Unclassified	SAR

NSN 7540-01-280-5500

Standard Form 298 (Rev. 2-89)
Prescribed by ANSI Std. Z39-18
298-102

CLASSIFIED BY:
DECLASSIFY ON:

Table of Contents

Section | **Page**

List of Illustrations

Figure **Page**

Network Identification Performance: (1) Simulations for the Middle East/North Africa, and (2) Maximum Likelihood Estimates of Teleseismic m_b for the GSETT-3 Primary Network

Terrance G. Barker

1. Simulations for the Middle East/North Africa

1.1 Introduction

We have simulated the detection and identification performance of the current and proposed IMS seismic networks in the Middle East/North Africa. Figure 1 shows a map of Africa and western Eurasia with the current IMS alpha stations and the area for which the simulations were done. The identification performance of a network is strongly dependent upon regional source and propagation variability. However, knowledge of those variations allow one to estimate their effects and to know that in some areas certain discriminants can work and in other areas they do not. Data sources included published results on wave propagation in this region and incorporated analyses of data taken by Vernon, *et al*, (1996) in Saudi Arabia.

1.2 IGPP Data Set and Regional Properties

We recently received data collected by Vernon, *et al.* (1996) on the Arabian Shield. The data were provided to us by Frank Vernon. Using the larger events in their data set for which there were magnitudes reported in the IMS Reviewed Event Bulletin, we extracted parameters which we used to make simulations for this region. The stations in their array and the events we analyzed are plotted in Figure 2. The IMS coverage currently is quite sparse in this region, so their data represents an important increment in knowledge there. In addition, the data set allows us to infer noise levels directly for stations on the shield.

Before analyzing specific events in the dataset, we examined the entire origin file to infer an approximate m_b threshold for the region. If the probability of detection is a Gaussian distribution $P(m_b; \mu,\sigma)$ with mean μ and sigma σ, then we assume the observed distribution follows

$$N_{inc} = P(m_b;\mu,\sigma)N_{occ}(m_b),$$
$$\log(N_{occ}) = a - b\log m_b$$

We further assume that b=1 and then fit the distribution of observed magnitudes, which were from IMS bulletins. Figure 3 shows the data and fit, with a=6.5, μ=4.5 and σ=0.3.

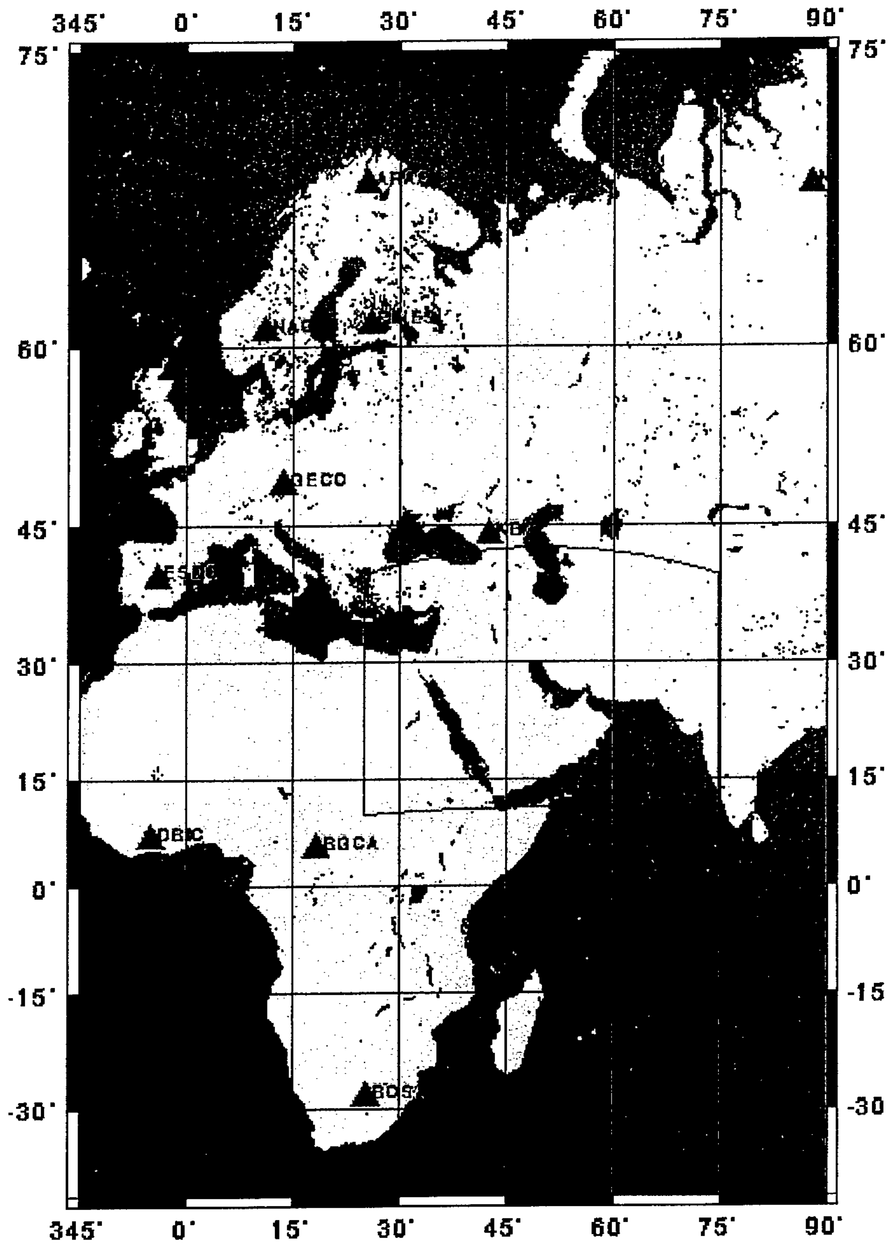

Figure 1. The current IMS network and the area for which the simulations were done.

Thus, the threshold for the IMS at the time these data were taken (late 1995 to early 1996) for the region as a whole was over m_b=4.5. By running simulations for that network we were able to set the scale factor in the P wave attenuation curves (effectively setting the relationship between moment and m_b).

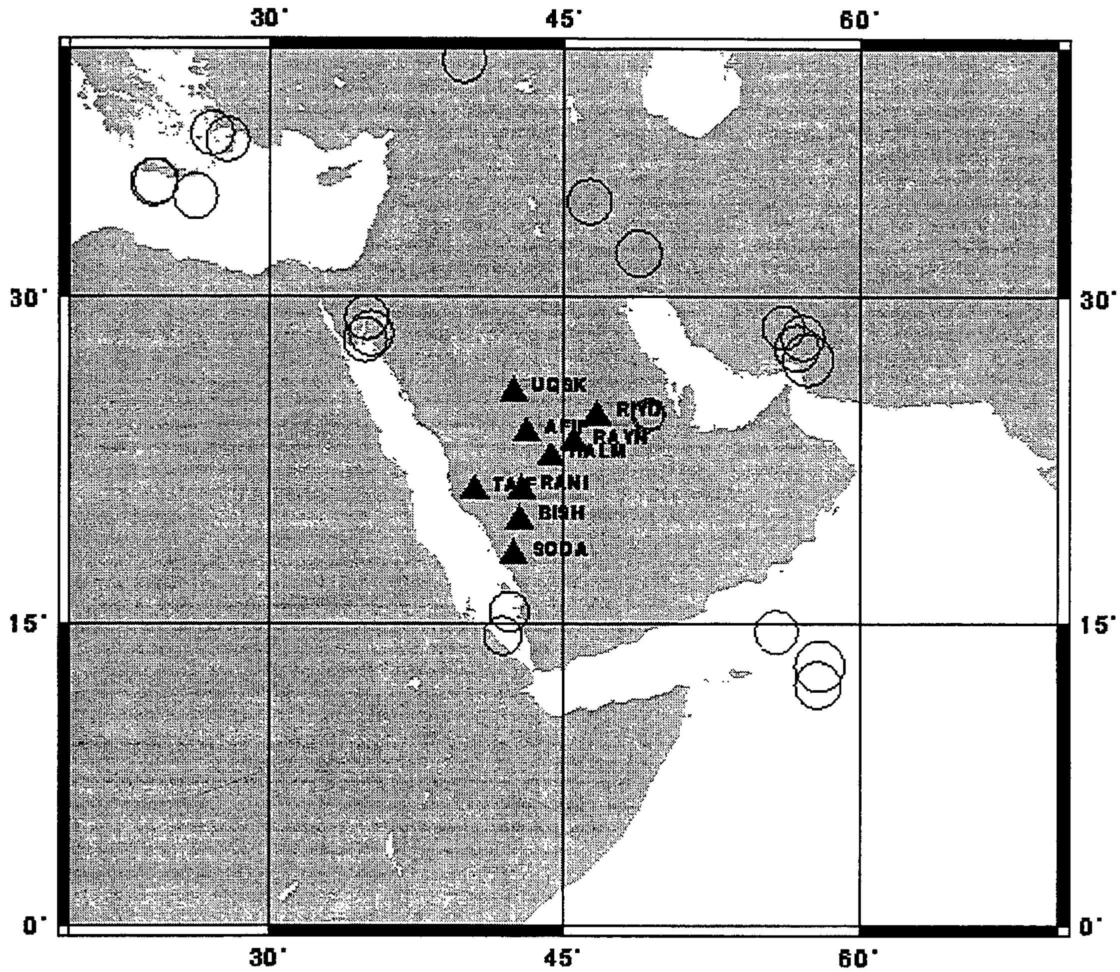

Figure 2. The network used by Vernon, *et al.* (1996) (solid triangles) and the locations of earthquakes (open circles) analyzed for this study.

Vernon, *et al.*, show that events in this region are very different in terms of their magnitude and relative amplitudes of regional phases. We selected events to represent five distinct areas, as suggested by Vernon, *et al.*, and measured time domain and spectral values. In order to source excitation levels, we calculated log(Lg/P) values and log amplitudes corrected to m_b=4 at a distance of 1000 km, relative to events in the NE Arabian Shield. That is,

$$\log A_{corr} = \log A_{obs}(mb,\Delta) + mb - 4 - 0.833\log(\Delta/1000) \qquad (1)$$

It would be preferable to relate the values to a long period measure, but long period spectral values (computed by us) from some of the areas were poor and/or there were not M_s values from each of the regions. It would also be preferable to calculate sub-regional values of Q(f), but this will be done by other institutions. Here, we assumed that values above 200 for Lg Q on the shield, near 200 off the shield and very low in the Red Sea. Table 1 shows the observed relative amplitudes.

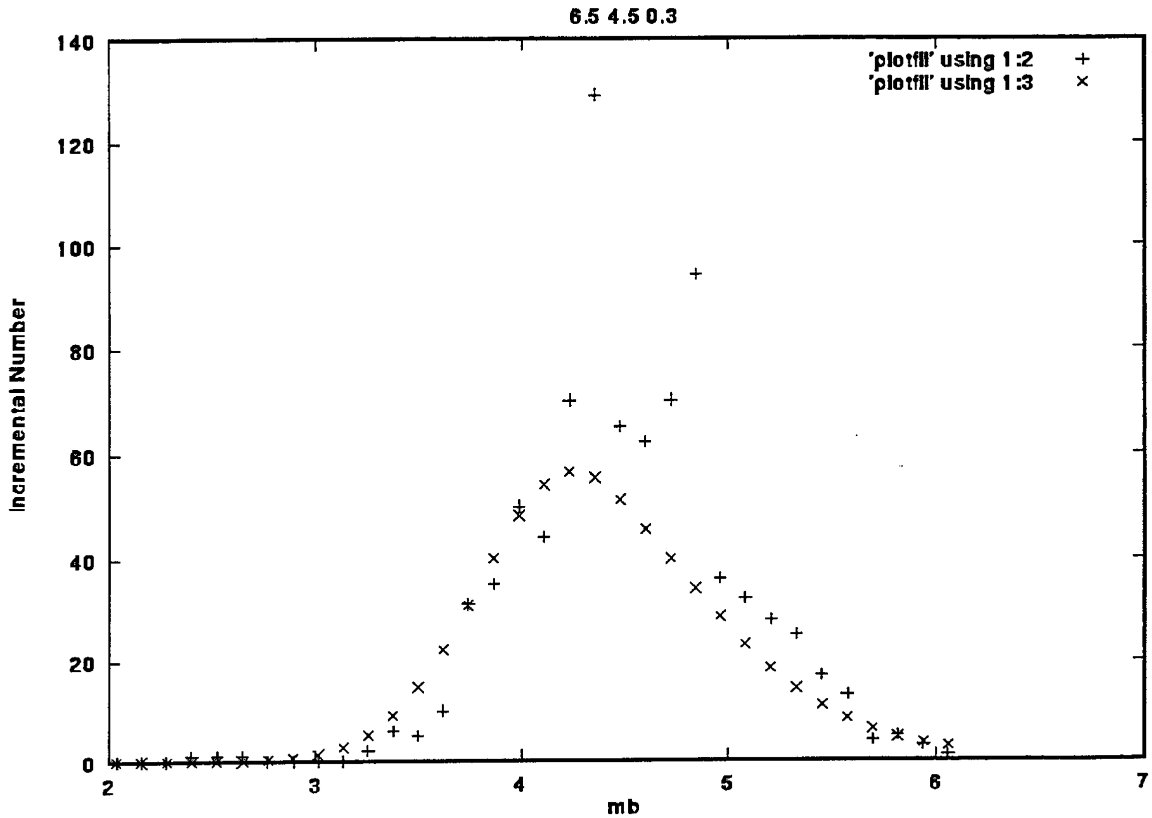

Figure 3: Observed distribution of events with m_b(+) and fit to the distribution(x).

Table 1. Observed Relative Amplitudes

Source region	Lg/P	A_{corr} for Lg	A_{corr} for Pn
NE Shield	0.3	0.	0
S. Red Sea	1	-0.8	-1.5
Aqaba	2	0.5	-1.1
Zagros	-0.3	-1.5	-0.9
Arabian Sea	0.4	-1	-1

The study region was made into a grid that represents differences in source and propagation properties as reported by Vernon, *et al.* and summarized by Sweeney (1995). The values of Table 2 and the other studies were used to populate the grid, which is shown in Figure 4.

For each of the grid members, we used relative amplitudes of signals from the sub-regions to set the regional parameters. In Xnice, the spectral amplitude of a regional phase at distance Δ has the form

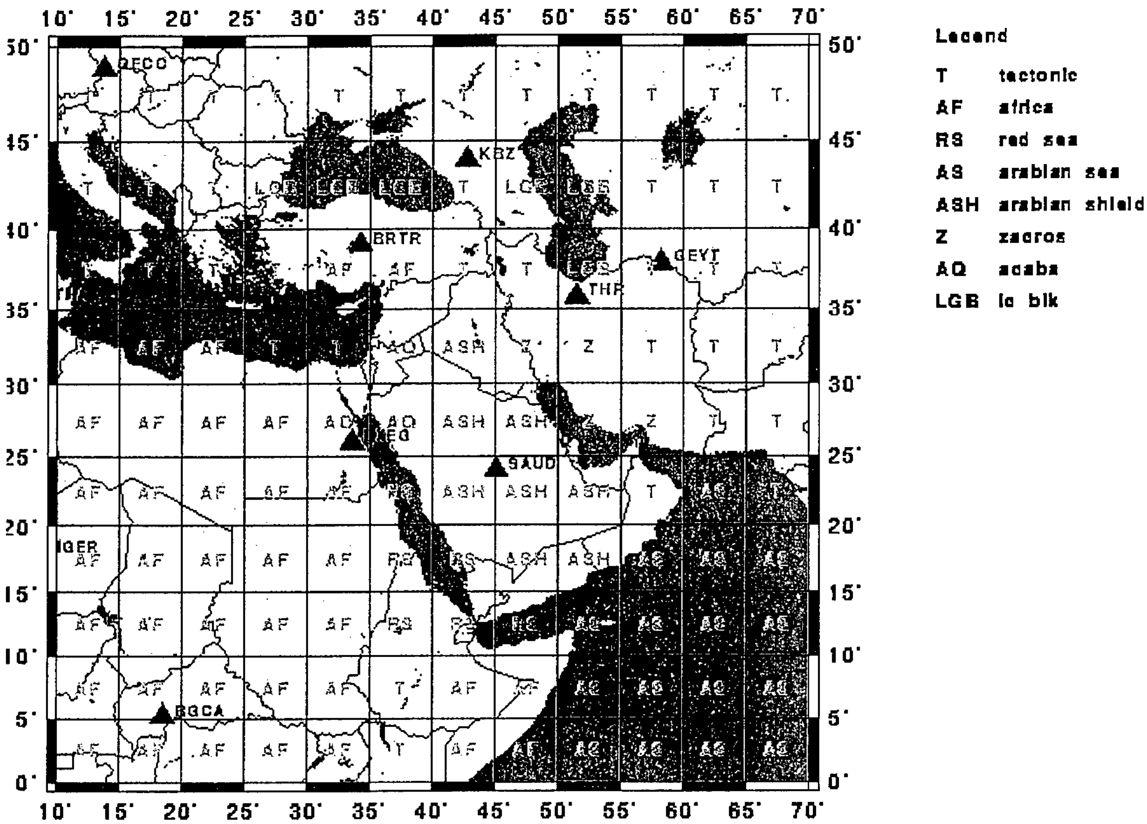

Figure 4. Grid of source and propagation parameters used in the simulations.

$$
\begin{aligned}
\log A_{eq} &= S_{eq}(f) + S_0 - 0.833\log(\Delta/\Delta_0) - 0.4342\gamma(\Delta-\Delta_0), \\
\log A_{ex} &= S_{ex}(f) + S_0 - 0.833\log(\Delta/\Delta_0) - 0.4342\gamma(\Delta-\Delta_0) + C_0^{\exp} + C_1^{\exp}\log(f),
\end{aligned} \tag{2}
$$

where $S_{eq}(f)$ and $S_{ex}(f)$ are the earthquake and explosion source spectra, and

$$\gamma = \pi f^{1-\eta} U_g^{-1} Q_0^{-1}.$$

Here, U_g is group velocity, Q_0 is the quality factor at 1 Hz, η is the slope of the Q versus frequency relation, S_0 is the source strength for unit moment, and C are the explosion relative source strength coefficients (see Barker, 1996 for details). The earthquakes generally occur in a narrow distance band (800 to 1100 km) from the network, so it was not possible to separate source and propagation factors from these data alone. We relied on the summary in Sweeney (1995) for Q values and used Baumgardt (1996) and Vernon, *et al.*, to deduce relative source strengths. There are no explosions in the data set, so we arbitrarily set $C_0^{\exp}$ to zero for Lg and to one for Pg and Pn. Since we could not reliably estimate $C_1^{\exp}$, we did not examine discrimination performance based on explosion spectral slope. The parameters used in the simulations discussed here are summarized in Table 2.

Table 2. Regional Source and Propagation Parameters

africa

Phase	U_g	Q_0	η	S_0	C_0^{exp}	C_1^{exp}
Lg	3500.	600.	0.39	-20.9	0.	-0.1
Pg	6000.	600.	0.39	-21.2	1.0	-0.5
Pn	8500.	600.	0.6	-21.2	0.8	-0.5

aqaba

Phase	U_g	Q_0	η	S_0	C_0^{exp}	C_1^{exp}
Lg	3500.	200.	0.39	-20.4		-0.1
Pg	6000.	200.	0.39	-22.4	-21.9	-0.5
Pn	8500.	200.	0.6	-22.4	-21.9	-0.5

arabian_sea

Phase	U_g	Q_0	η	S_0	C_0^{exp}	C_1^{exp}
Lg	3500.	200.	0.39	-21.9	0.0	-0.1
Pg	6000.	200.	0.39	-22.3	1.0	-0.5
Pn	8500.	200.	0.6	-22.3	1.0	-0.5

arabian_shield

Phase	U_g	Q_0	η	S_0	C_0^{exp}	C_1^{exp}
Lg	3500.	300.	0.39	-20.9	0.2	-0.1
Pg	6000.	300.	0.39	-21.2	1.4	-0.5
Pn	8500.	300.	0.6	-21.2	0.8	-0.5

lg_blk

Phase	U_g	Q_0	η	S_0	C_0^{exp}	C_1^{exp}
Lg	3500.	5.	0.45	-21.7	0.4	-1.1
Pg	6000.	10.	0.68	-22.7	0.8	-0.1
Pn	8500.	10.	0.8	-22.7	2.2	-0.1

red_sea

Phase	U_g	Q_0	η	S_0	C_0^{exp}	C_1^{exp}
Lg	3500.	40.	0.45	-21.7	0.0	-1.1
Pg	6000.	40.	0.68	-22.7	1.0	-0.1
Pn	8500.	40.	0.8	-22.7	1.	-0.1

tectonic

Phase	U_g	Q_0	η	S_0	C_0^{exp}	C_1^{exp}
Lg	3500.	671.	0.43	-21.2	0.3	-1.1
Pg	6000.	1000.	0.39	-21.5	1.4	-0.1
Pn	8500.	500.	0.6	-21.5	0.8	-0.1

zagros

Phase	U_g	Q_0	η	S_0	C_0^{exp}	C_1^{exp}
Lg	3500.	200.	0.39	-22.6	0.0	-0.1
Pg	6000.	200.	0.39	-22.3	1.0	-0.5
Pn	8500.	200.	0.6	-22.3	1.0	-0.5

1.3 Noise Levels of Saudi Stations

For the simulations used here, we used time series from the IGPP data set to find noise levels for the proposed SAUD station. The Saudi stations are very quiet, as can be seen from Figure 5, which shows representative noise spectra for five stations on the same day, plus the low noise model proposed by Peterson (1993). The station noise levels are comparable to the low noise model, with the noise at station HALM significantly lower.

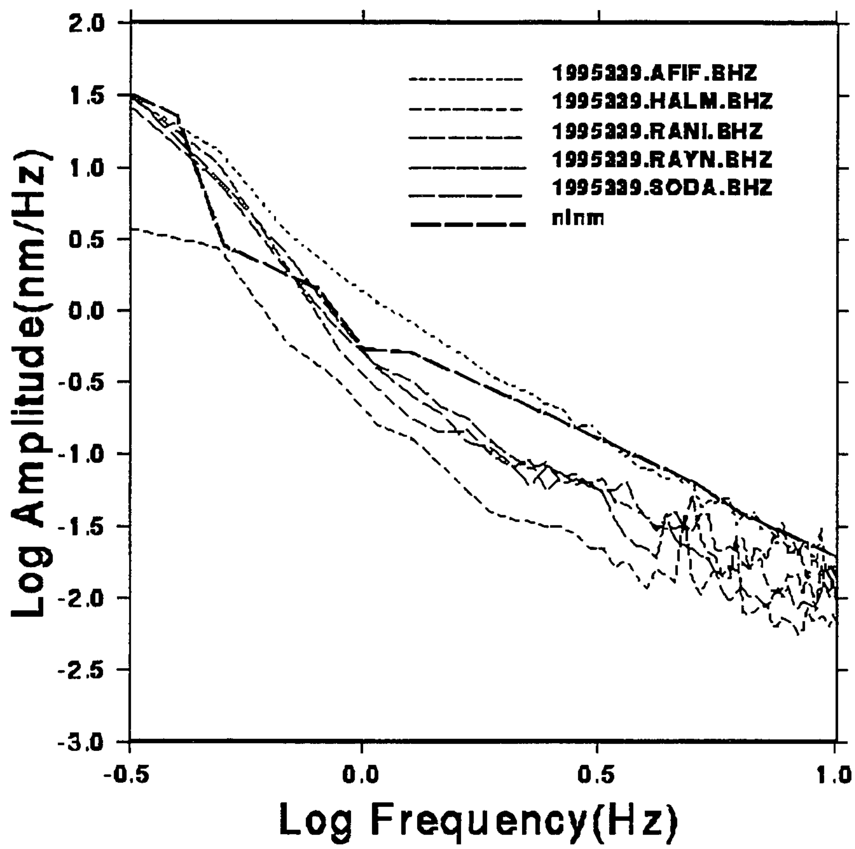

Figure 5. Noise spectra for five Saudi stations on the same day (1995339), plus the low noise model proposed by Peterson (1993).

1.4 Simulations of Detection and Identification Performance

The IMS network proposed by the Conference on Disarmament Experts working Group in August, 1995 is more dense in the Middle East (Figure 6) than that which is currently in place. In the following we compare estimates of the performance of the existing network with the proposed net. We begin with the detection thresholds.

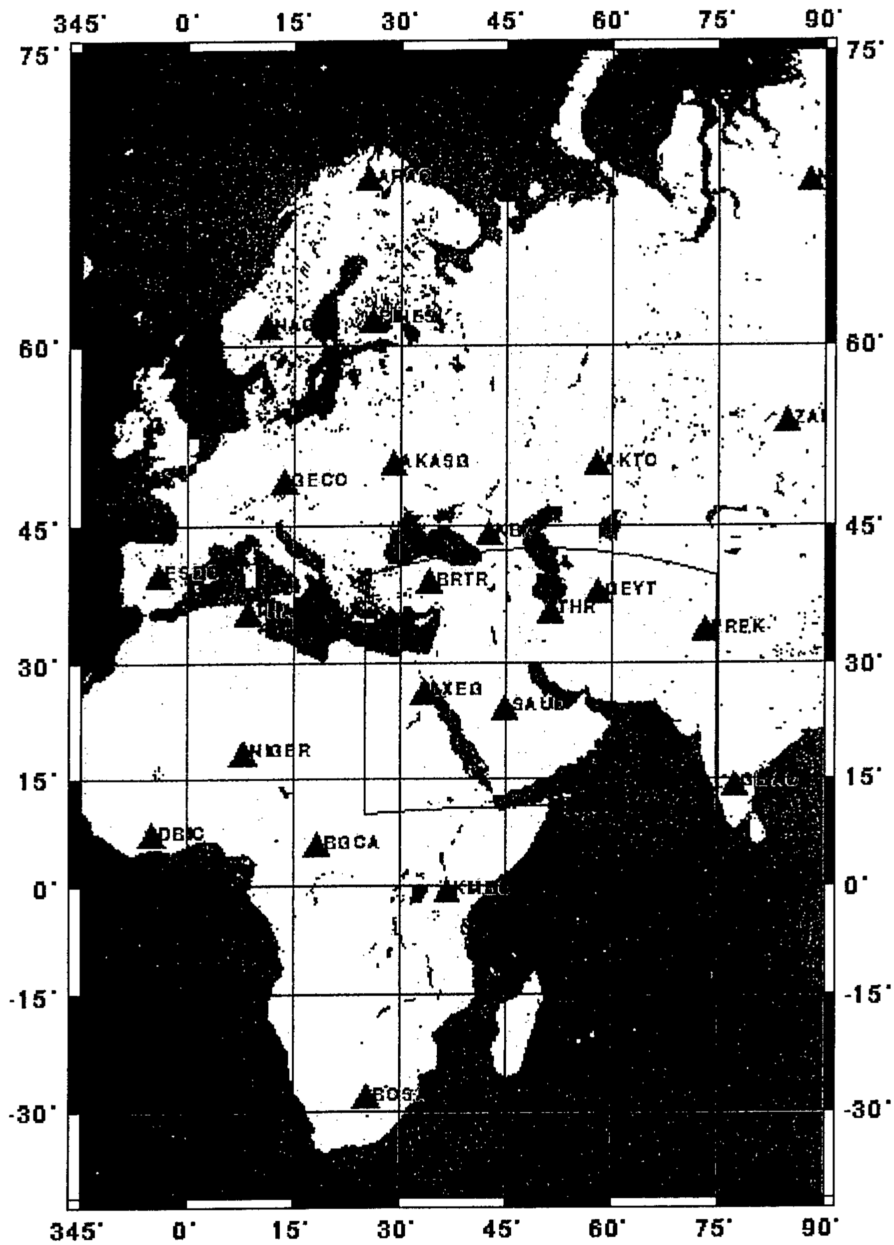

Figure 6. Proposed IMS seismic stations.

Contours of m_b detection thresholds for the current network are shown in Figure 7. By detection, we mean the criteria used in GSETT-3 and currently implemented on the IMS. The rules are based on a weighted sum of measurements (J. Carter, Center of Monitoring Research, personal communication):

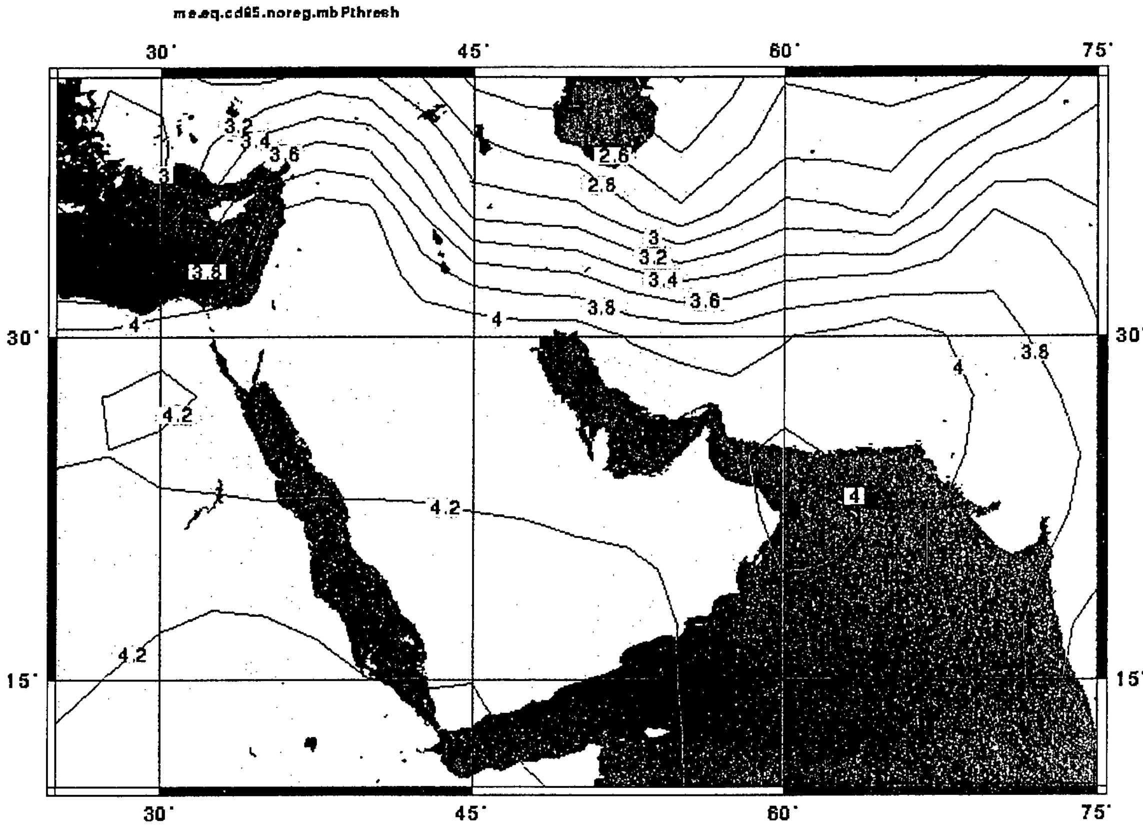

Figure 7. Contours of m_b detection thresholds for the current network.

Table 3. Weights for Measurements in Determining Detection Status

Primary Time	1.0
Secondary time	0.7
Array azimuth	0.4
Array slowness	0.4
Single station azimuth	0.2
Single station slowness	0.2

Her, "primary" refers to teleseismic P or regional Pg or Pn and secondary refers to teleseismic pP or S or regional Lg. All azimuths are determined from P, Pg or Pn. A sum is formed from the number of measurements which exceed the signal-to-noise ratio times their respective weights for the stations in the network. An event is considered detected if the sum exceeds 3.55. Thresholds in this figure and in the remainder of this report are 90% confidence values.

The thresholds decrease dramatically towards the NE as coverage improves. For events on the Arabian peninsula, detections are teleseismic (no stations are within the regional cutoff distance of 20 degrees). The detection thresholds for the proposed network are shown in Figure 8.

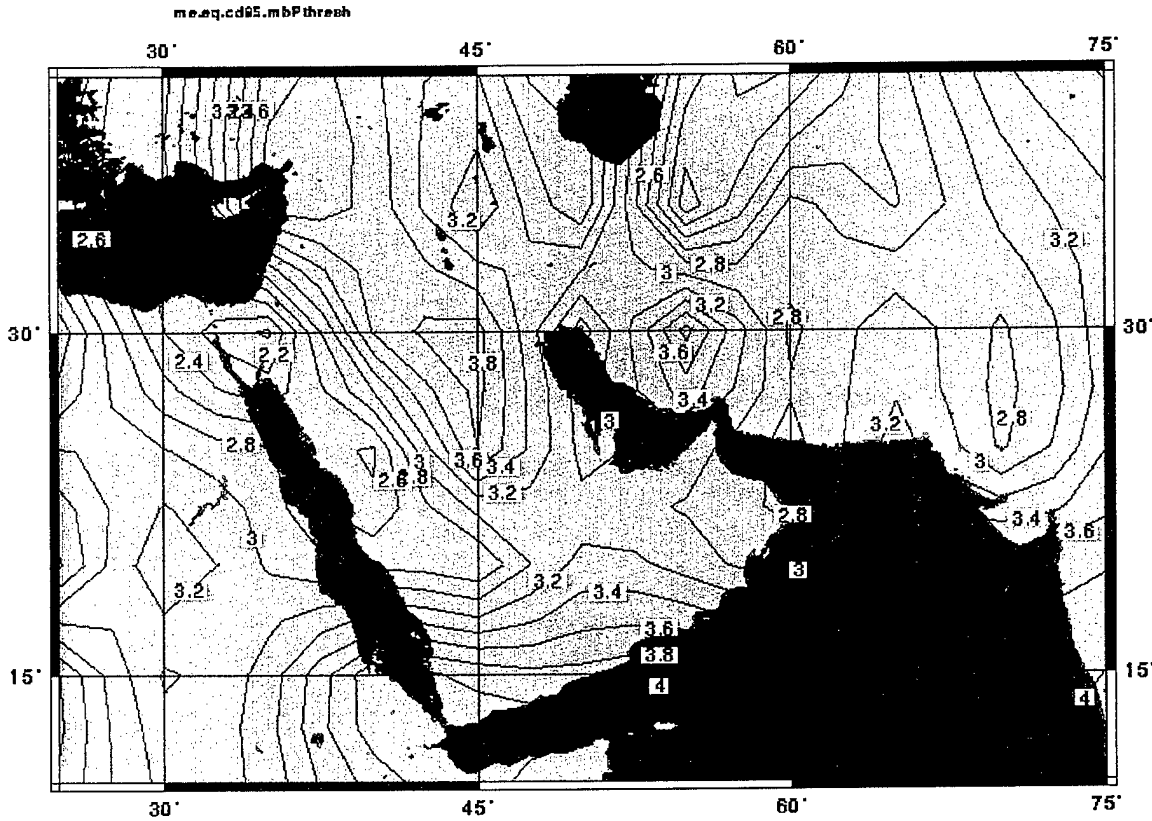

Figure 8. Contours of m_b detection thresholds for the proposed IMS network.

The additional stations lower the detection threshold substantially. Variability within the region is due to station geometry and variations in source strength and propagation parameters (Tables 1 and 2, Figure 4).

We turn now to identification performance. We note first that teleseismic discriminants are ineffective because events in this region (and the simulation) are typically shallow (<10 km). We did not model the M_s:m_b discriminant because we need accurate estimates of long-period noise for the networks, which we currently do not have. Thus, for events occurring on-shore, we must rely on regional discriminants for identification. Since there are no events detected (in the sense of the rules in Table 3) by the current IMS network in this region, discrimination cannot be done. On the other hand, the proposed network is capable of regional discrimination. We consider first the Lg/P discriminant. An event is considered identified as an earthquake if (1) the event satisfies the event detection criterion (Table 1), (2) both Lg and Pn or Pg exceed the signal-to-noise ratio at least 1 station, and (3) the Lg/P ratio exceeds a specified value. Figure 9 shows the contours of m_b(Lg) threshold.

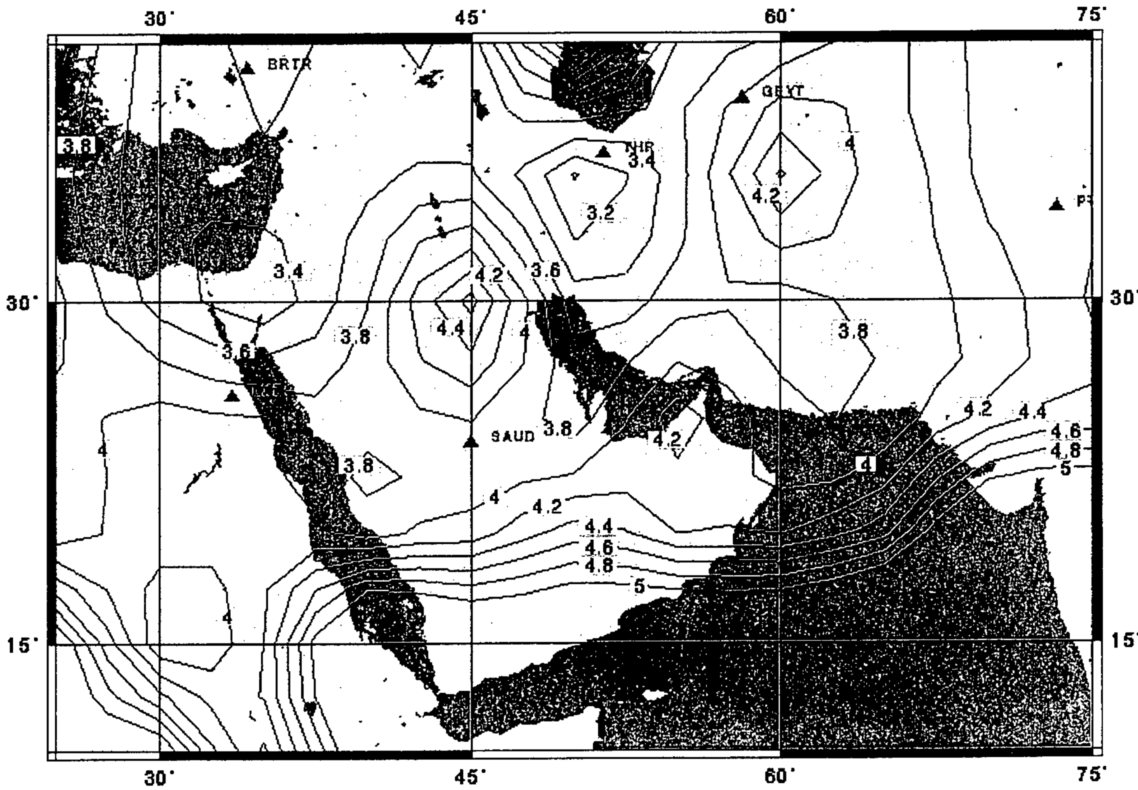

Figure 9. Contours of $m_b(Lg)$ detection thresholds for the proposed IMS network.

Note that to the north of SAUD, the $m_b(Lg)$ threshold increases locally, This is due primarily to the reduced excitation of Lg (see Table 1) towards the Zagros propagation grid zones. We can see the influence of the excitation levels S_0 on $m_b(Lg)$ from Figure 10, which shows contours those levels. In general, where the excitation is high, the threshold is low, and vice-versa. In addition to the detection of Lg, the Lg/P ratio must exceed a specified level. We show in Figure 10, contours of observed Lg/P, which are low towards the Zagros region, and high in the Gulf of Aqaba. We would thus expect from Figures 10 and 11 for the Lg/P ratio to identify earthquakes as such most successfully near the Gulf of Aqaba and least near the Zagros. Indeed this is the case, as seen in Figure 12 where we have plotted contours of the fraction of events with log(Lg/P) > 0 at m_b=3.5. The fractions are generally high where the observed Lg/P ratios are high, except in regions where the $m_b(Lg)$ threshold is high, as in the NE part of the Arabian peninsula. The fraction of identified events is near one if we plot them at m_b=4.0, as shown in Figure 13. The values are still around 0.6 in the southern Red Sea, due to poor propagation and local values of log(Lg/P) around 0.

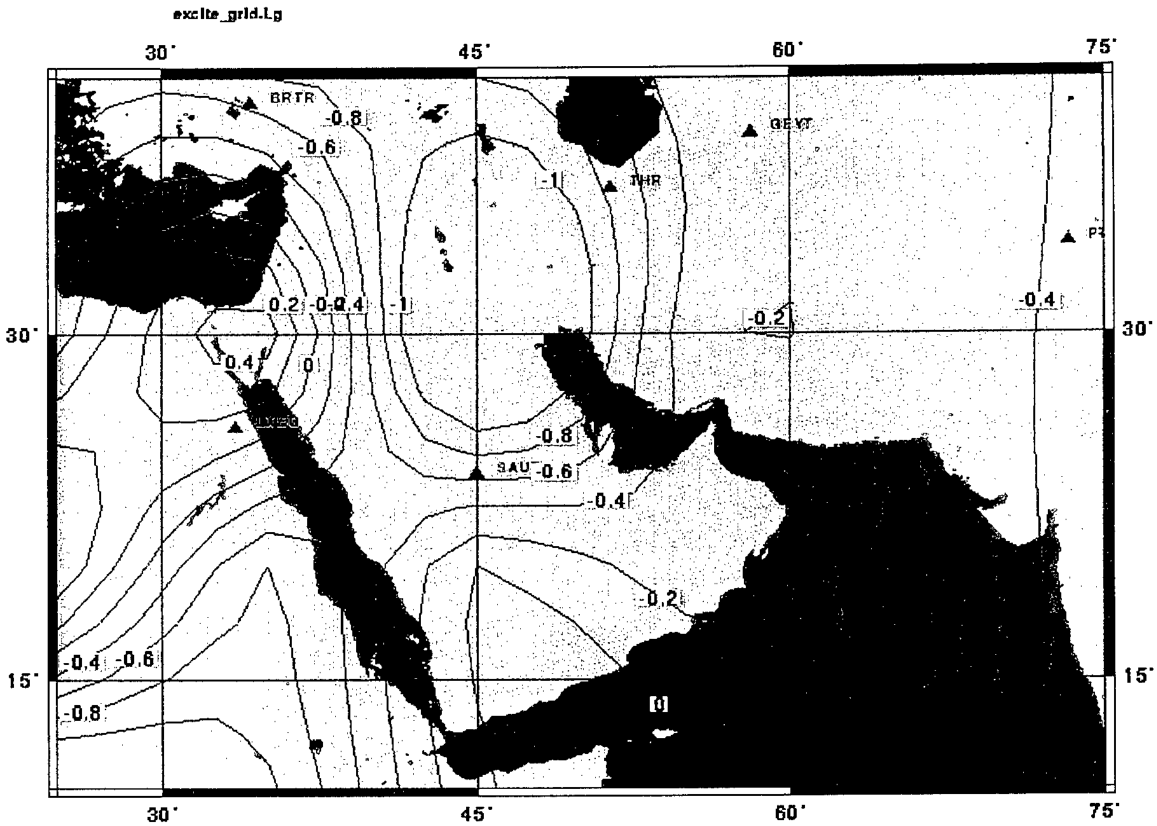

Figure 10. Contours of $m_b(Lg)$ excitation levels S_0.

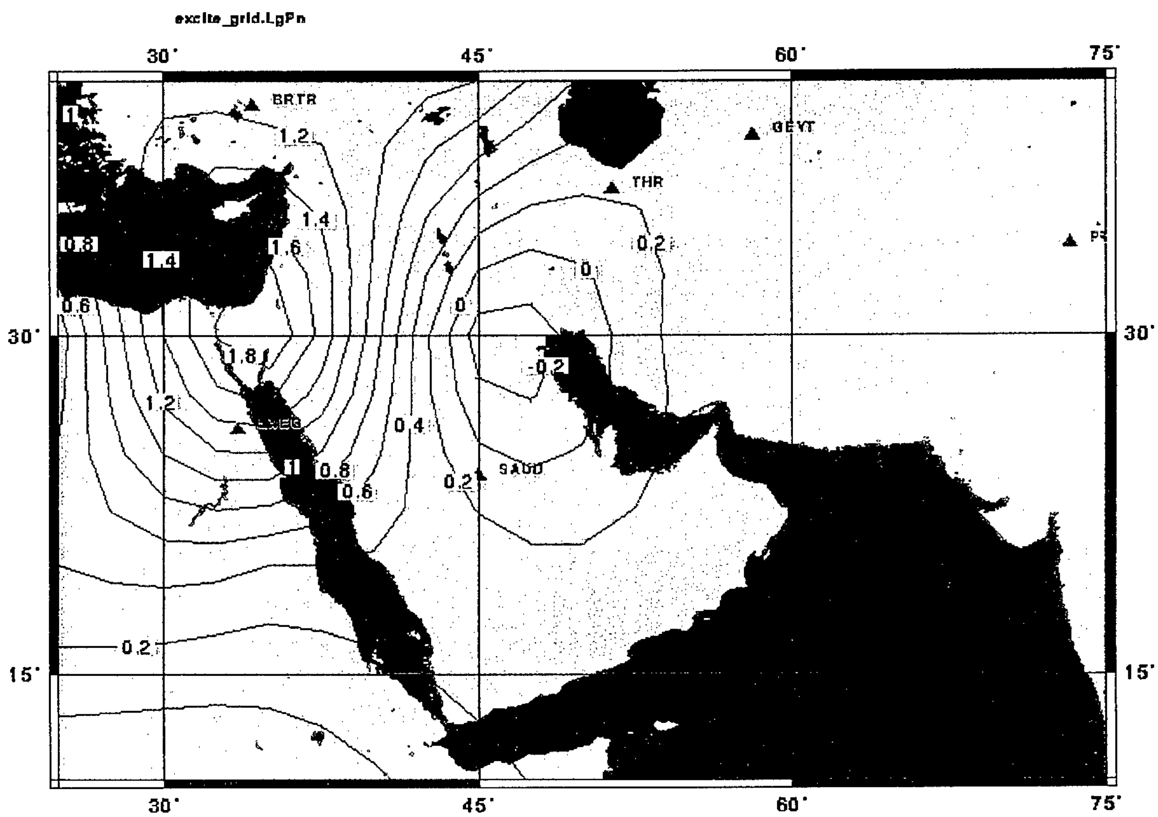

Figure 11. Contours of Lg/P ratio.

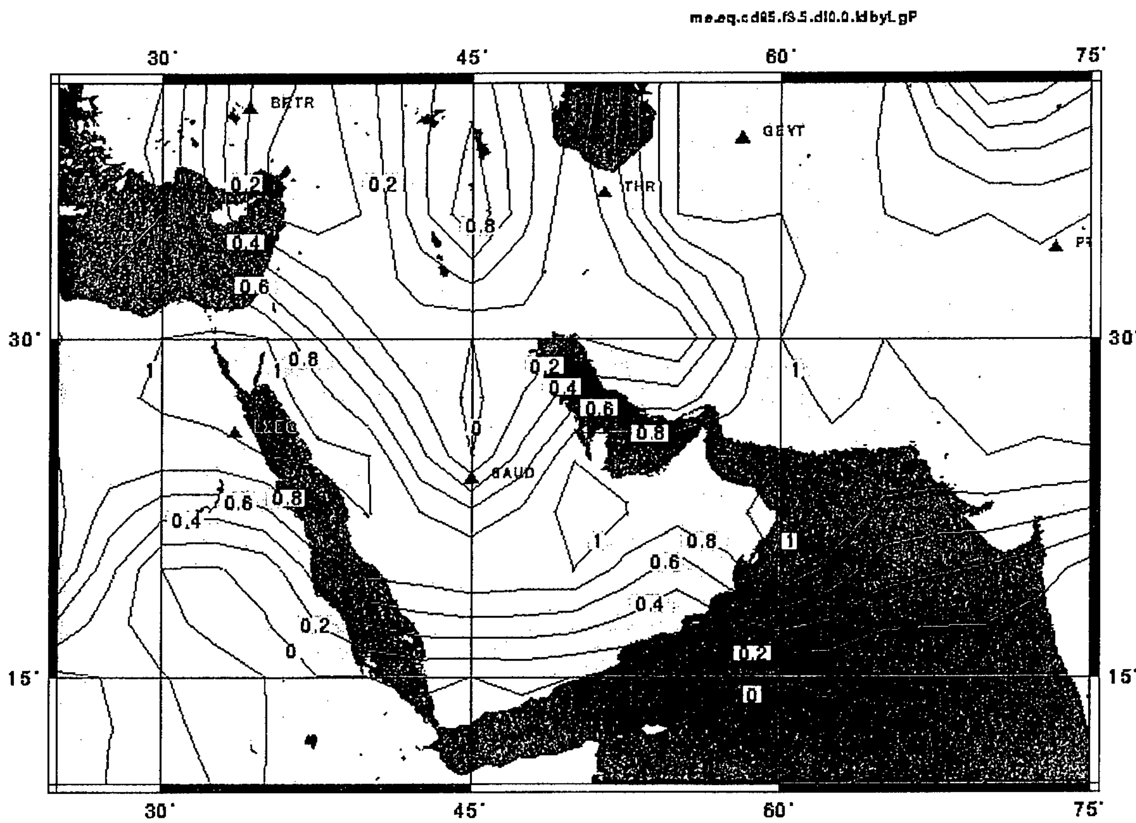

Figure 12. Contours of fraction of events identified as earthquakes by the Lg/P discriminant at m_b=3.5 for the proposed IMS network. The decision line is log(Lg/P) = 0.0.

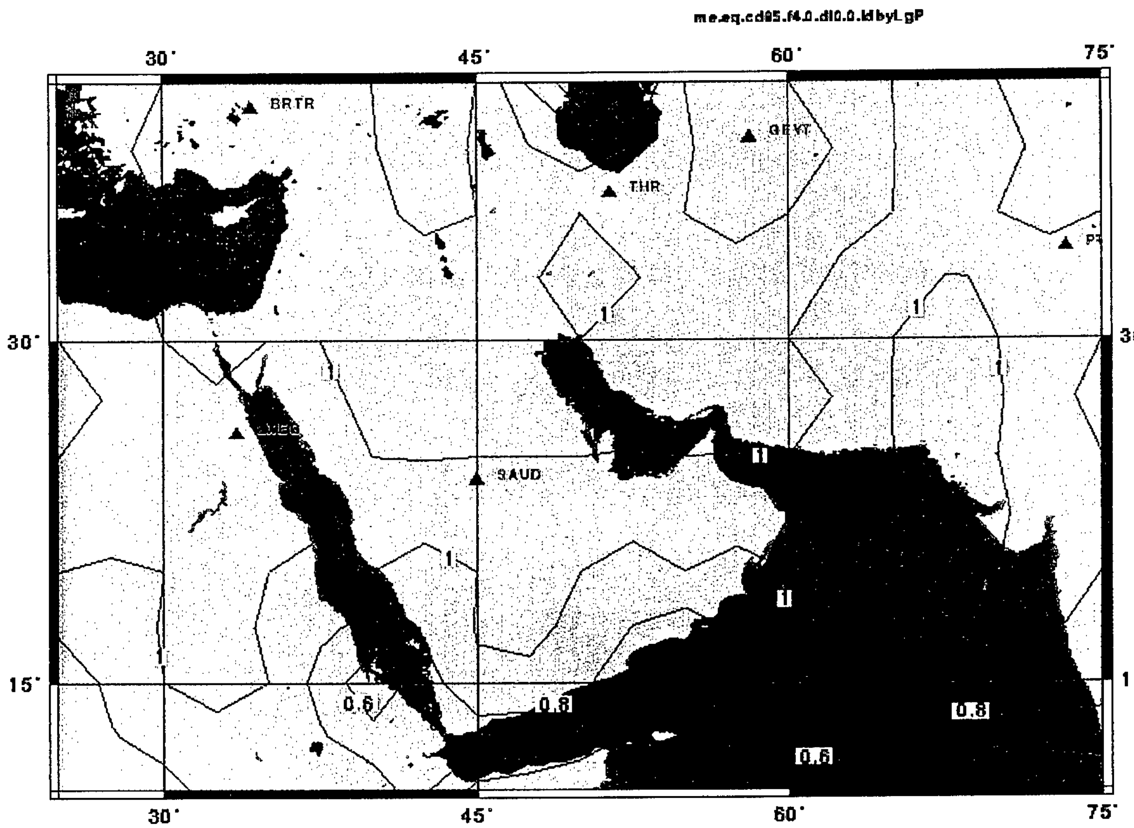

Figure 13. Contours of fraction of events identified as earthquakes by the Lg/P discriminant at m_b=4.0 for the proposed IMS network. The decision line is log(Lg/P) = 0.0.

We do not currently have adequate excitation and propagation information at higher (>6 Hz) to accurately simulate the regional (Lg or Pg/Pn) spectral slope discriminants. We can, however, address whether higher frequency signals could be detectable on the Arabian shield using noise spectra obtained from series preceding signals in Vernon's database. These stations are very quiet (Figure 5). Using the propagation parameters in Table 2 and a standard earthquake source model (Brune, 1970), we find that the higher frequency signals exceed the noise out to 10 Hz (even though signal power is decaying with frequency, the noise is decaying faster). That is, At locations where events can be detected at one Hz, they can generally be detected at ten Hz. If the station planned for Saudi Arabia is comparable to Vernon's stations, the spectral slope discriminants can be applied on the Arabian shield.

Each of the stations proposed in this region is very important to identification performance. Due to lack of coverage to the SE of SAUD (in the Arabian Sea), this station is essential for monitoring the Arabian shield and the Sanai peninsula. Without station LXEG, there are no regional detections in NE Africa and stations THR and BEYT are needed for regional detections south of the Caspian Sea.

2. Maximum Likelihood Estimates of Teleseismic m_b for the GSETT-3 Primary (Alpha) Network

2.1. Introduction

The maximum likelihood estimates of magnitude (Ringdal, 1976) was developed to improve measures of signal amplitudes when are below detection levels in some or all of the network As pointed out by Von Seggern and Rivers (1978), values of m_b derived from arithmetic mean tend to have a positive bias, which may be eliminated by the use of maximum likelihood estimates. In the following, we simulate a suite of earthquakes recorded at the GSETT-3 Alpha network, and compare the m_b's computed using the two methods with true values.

2.2 Simulations

The simulations described here use the Xnice program, described in detail in Barker, 1996. In the following, we specify parameters specific to this problem and refer the reader to that document for methods, models and other parameters.

2.2.1. Source Properties

So that a realistic geographic distribution of events is simulated, we extracted event locations from the Late Events Bulletin for 1993 to 1996 from the prototype IDC. This included about 20,000 events. Seismic moments were then distribution followed the rule

$$\begin{aligned} &\log N_{cum} = 2.85 - \log M_0, \\ &\log M_0 \geq 15, \end{aligned} \tag{3}$$

where N_{cum} is the cumulative number of events with moment $\geq M_0$ (note that in Xnice a moment distribution is specified, rather than a magnitude). The stress drop were governed by log-normal distribution with a mean of 10 MPa (100 bars) and standard deviation of 5 Mpa.

2.2.2 Propagation Parameters

Amplitude tables are from the Vieth and Claussen tables. Random errors in log amplitude of teleseismic P due to propagation followed a log-normal distribution with zero mean and 0.28 log-units standard deviation.

2.2.3 GSETT-3 Primary Station Network

The 41 stations used in this simulation, their location and mean log noise amplitude (microns) at 1 Hz are given the following table:

Station	Latitude	Longitude	Noise
AKT	50.434	58.018	-3.147
ARA0	69.535	25.506	-2.156
ASAR	-23.666	133.905	-2.774
BDFB	-15.633	-48.000	-2.899
BGCA	5.176	18.424	-3.349
BJT	40.018	116.168	-3.064
BOSA	-28.613	25.416	-2.726
CMAR	18.824	98.947	-2.920
CPUP	-26.331	-57.329	-2.919
DBIC	6.670	-4.856	-3.147
ESDC	39.675	-3.965	-2.751
FIA0	61.444	26.079	-2.488
GEC0	48.836	13.704	-3.147
HFS0	60.134	13.696	-2.814
KBZ	43.950	42.683	-3.147
LBNH	44.240	-71.930	-2.375
LOR	47.268	3.859	-2.618
LPAZ	-16.288	-68.131	-3.552
MAW	-67.604	62.871	-2.303
MBC	76.242	-119.360	-3.347
MIAR	34.546	-93.573	-2.868
MJAR	36.542	138.207	-2.891
NAO	61.040	11.215	-2.450
NPO	64.771	-146.886	-2.007
NRI	69.400	88.000	-3.179
PDAR	42.780	-109.560	-3.315
PDY	59.600	112.500	-3.073
PFCA	33.610	-116.460	-3.005
PLCA	-40.731	-70.550	-2.955
SCHQ	54.817	-66.783	-2.735
SPITS	78.180	16.370	-1.583
STKA	-31.882	141.592	-2.813
TXAR	29.334	-103.667	-3.243
ULM	50.250	-95.875	-3.015
VNDA	-77.519	161.846	-2.780
WALA	49.056	-113.911	-2.983
WHY	60.695	-134.967	-2.840
WOOL	-31.073	121.678	-2.919
WRA	-19.944	134.341	-3.020
YKA	62.493	-114.605	-3.433
ZAL	53.940	84.805	-3.463

The GSETT-3 Primary network of stations has a wide range of short-period noise levels ranging from a high of -1.6 (0.025 microns) to low values of -3.5 (0.003 microns).

2.3 Results

Figure 14 shows the locations of stations and events used in the simulations. In Figure 15, we have plotted arithmetic mean m_b's (m_b^{am}) versus $\log M_0$. Only those events which meet the GSE detection criteria are included. Also plotted in this figure is the ensemble average of the values of m_b within 0.125 of the plotted $\log M_0$ (the averages are indicated by x's). A third set of values on the figure are the values of m_b when there is no propagation variation or ground noise and no statistical variation in the stress drop. We refer to these values as the "true" values. The curvature is due to the change in corner frequency with moment. We see that m_b^{am} exceed the true values by about 0.5 at the lowest magnitudes and approach the true value at higher m_b. Figure 16 shows a comparable plot for maximum likelihood estimated m_b (m_b^{mle}). The values of m_b^{mle} are quite close to the true values across the magnitude range. m_b^{am} and m_b^{mle} are plotted against each other in Figure 17, which shows that the m_b^{am} exceed the m_b^{mle}, in agreement with Von Seggern and Rivers (1978).

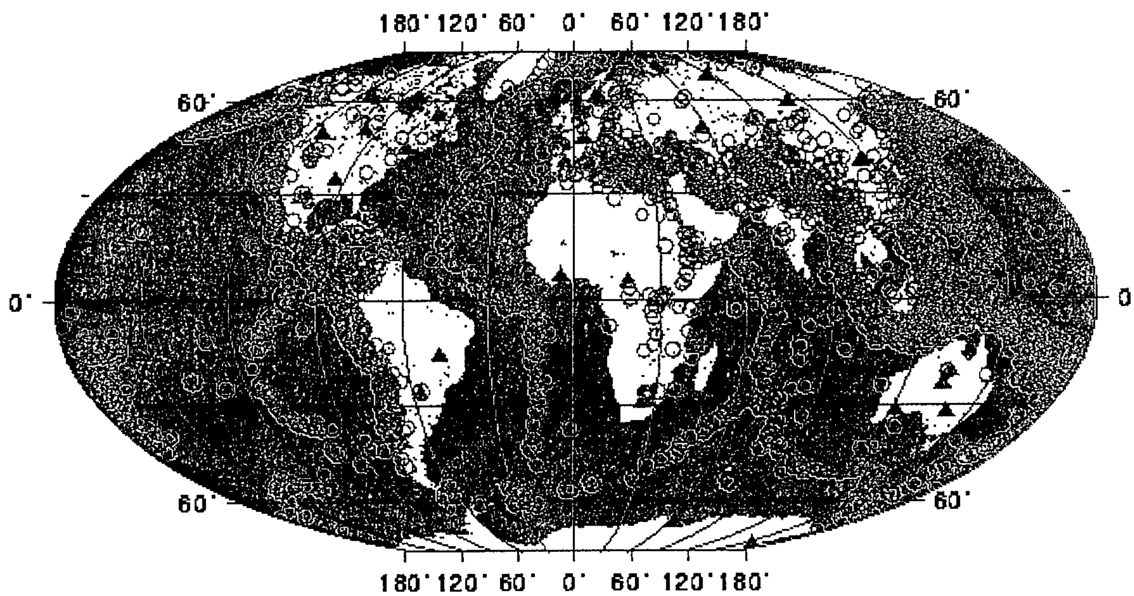

Figure 14. Locations of stations (triangles) and events (circles) used in the simulations.

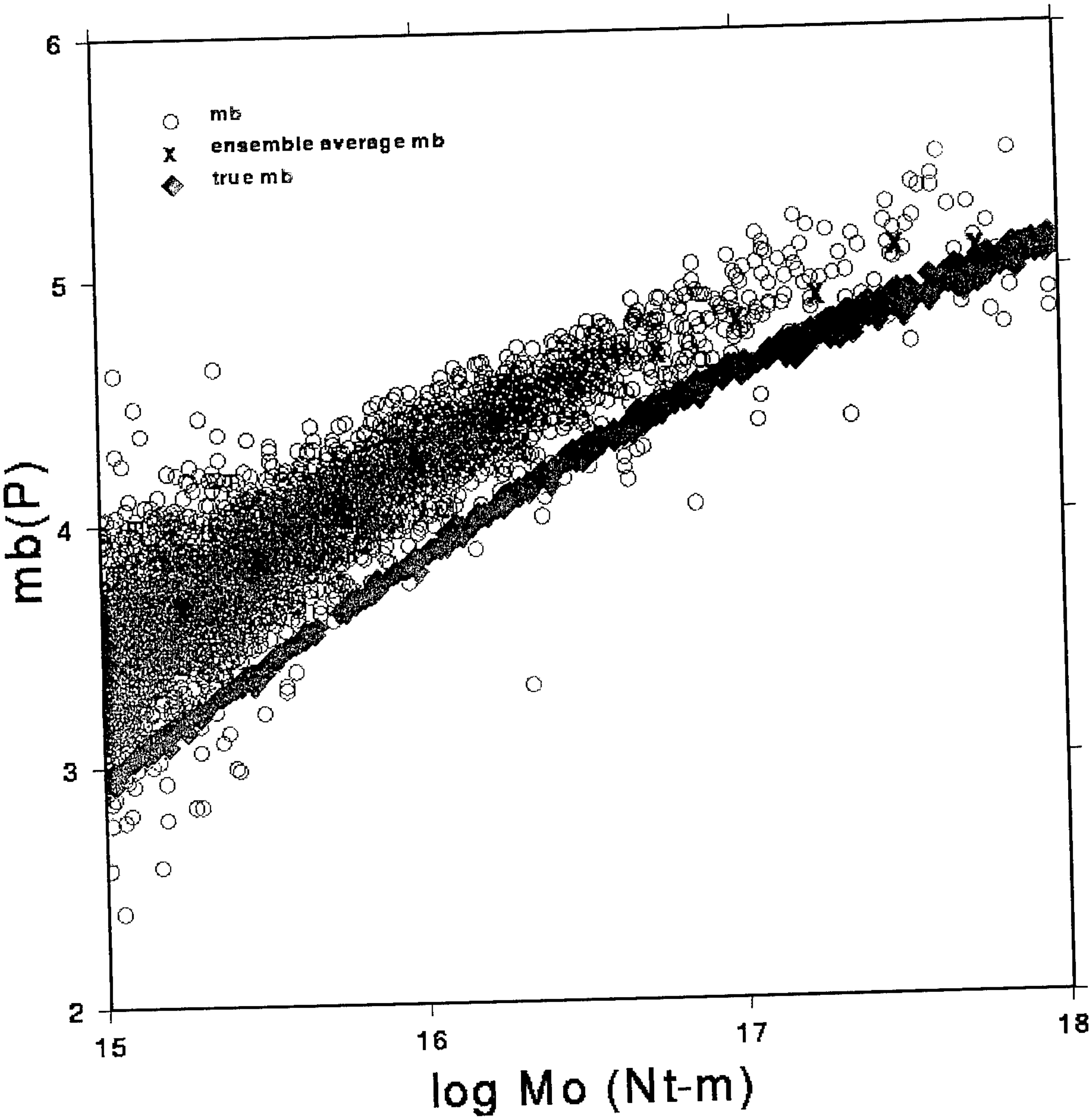

Figure 15. Arithmetic mean m_b (circles), ensemble average $m_b(x)$ and true m_b (diamonds) are plotted versus log(moment).

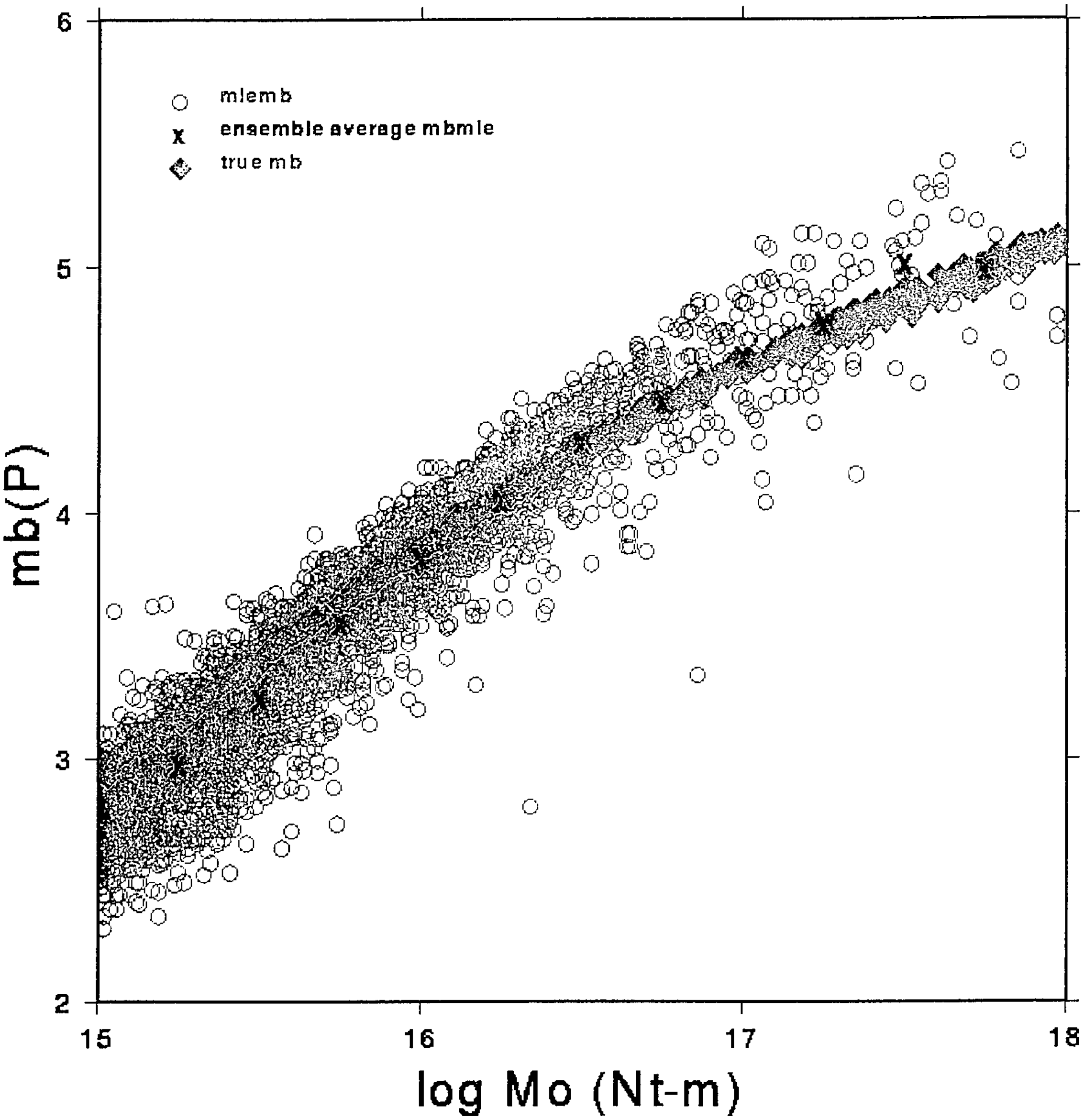

Figure 16. Maximum likelihood estimate m_b (circles), ensemble average $m_b(x)$ and true m_b (diamonds) are plotted versus log(moment).

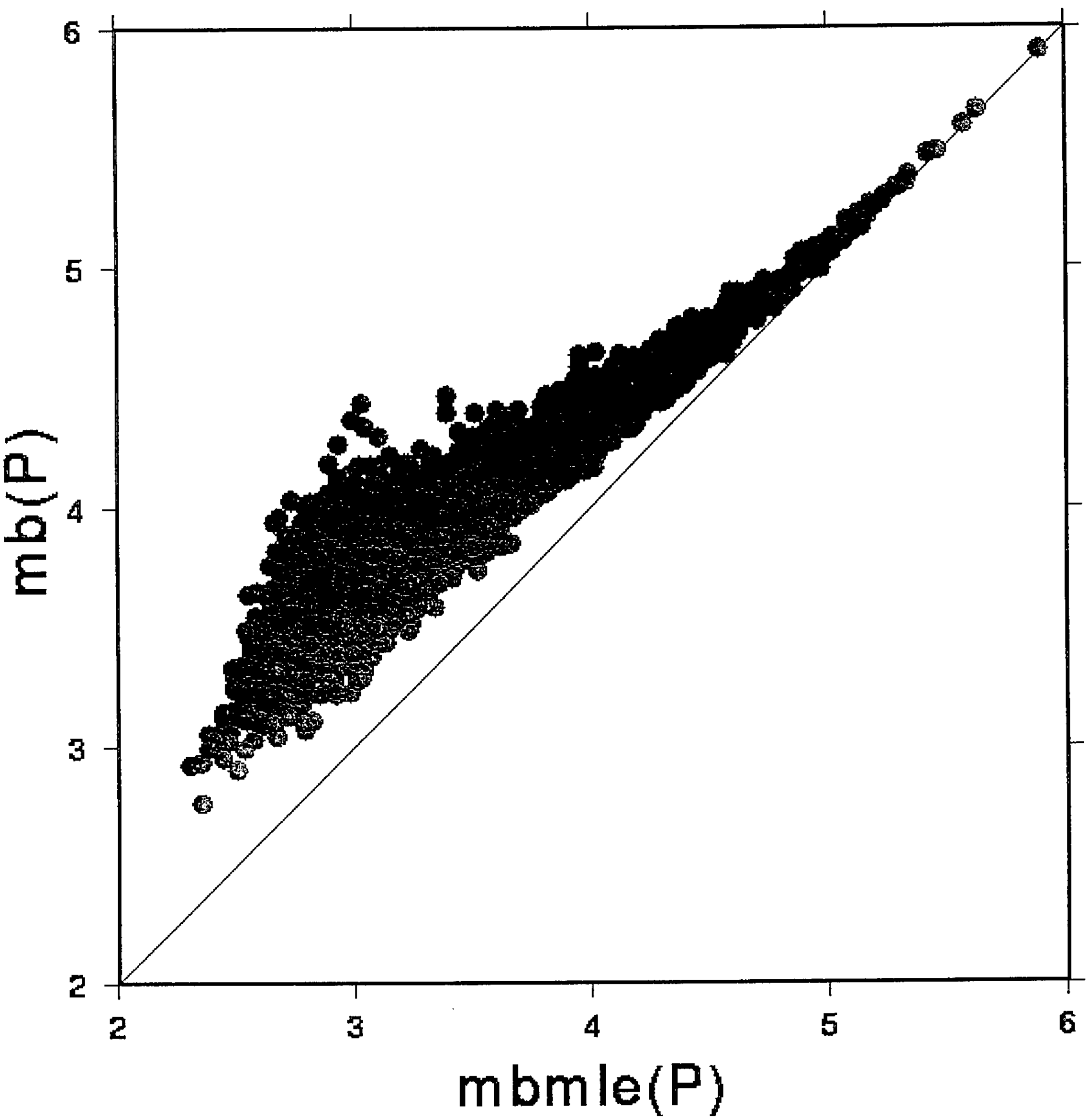

Figure 17. Arithmetic mean m_b are plotted against maximum likelihood estimate m_b.

The incremental number of events versus m_b^{mle} and m_b^{am} are shown in Figure 18. In each case the values are normalized by the total number of events detected. The peak number of events for m_b^{mle} occurs at a lower value than m_b^{am}, indicating an apparent lower detection threshold for m_b^{mle} . The cumulative numbers (number with values greater than m_b) are shown in Figure 19. Also shown on this figure are the true values. The slope of the m_b^{mle} distribution at high magnitudes (from which a "b value" would be measured) has about the same value as the slope of the true values, while the m_b^{am} distribution has a greater slope. Note that the slope is greater than one (the slope of the log moment distribution above) due to corner frequency effects.

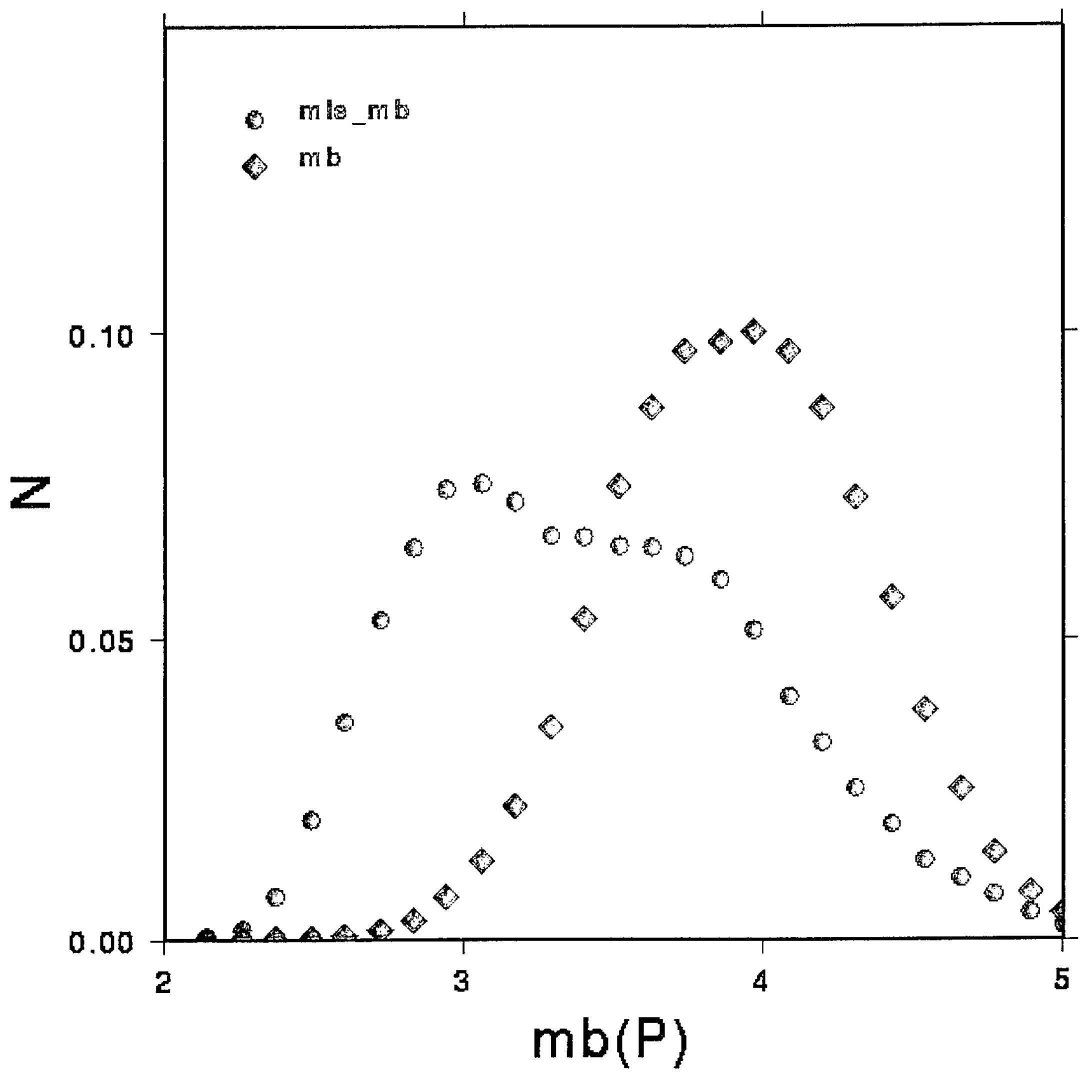

Figure 18. Incremental number of events versus m_b^{mle} (circles) and m_b^{am} (diamonds).

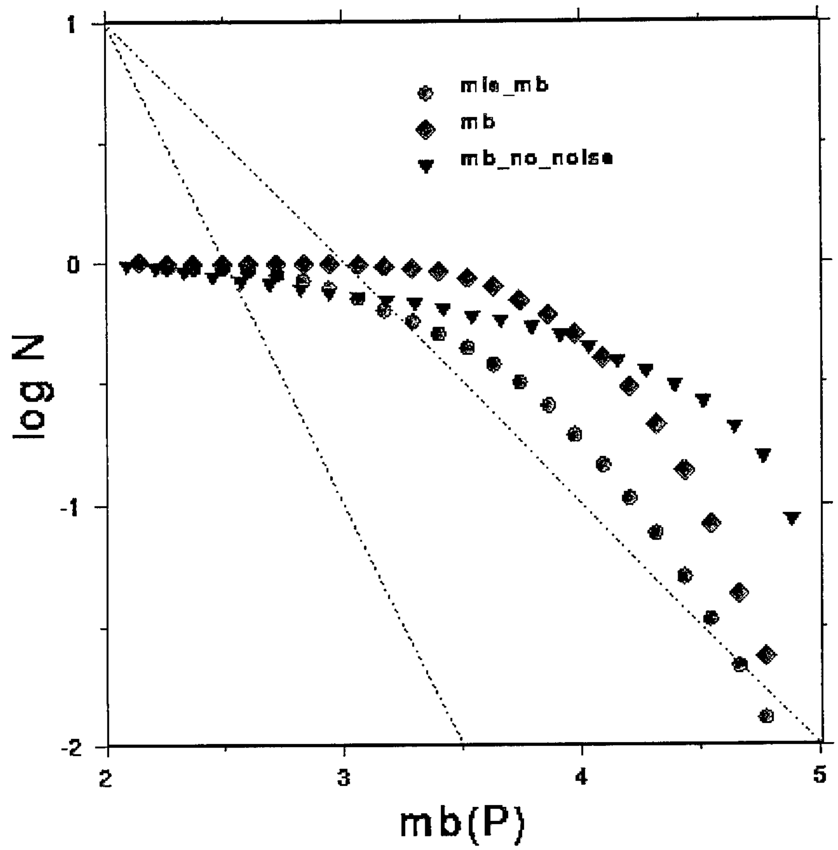

Figure 19. Cumulative number of events versus m_b^{mle} (circles) and m_b^{am} (diamonds) and true m_b (inverted triangles). Straight dashed lines have slopes of -1 and -2.

These results indicate that replacement of m_b^{am} with m_b^{mle} as the network m_b values in future bulletins will reduce magnitude bias at low magnitudes and decrease the slope of the cumulative distribution of events versus m_b in accordance with conventional wisdom.

3. References

Barker, T. G. (1996), "Xnice: A System for Assessing Network Identification Performance," S-CUBED Scientific Report No. 2 to Phillips Laboratory, PL-TR-96-2087.

Baumgardt, D. R. (1996), "Characterization of Regional-Phase Propagation and Seismic Discriminants for the Middle East," *Proceedings of the 18th Annual Seismic Research Symposium on Monitoring a Comprehensive Test Ban Treaty*, edited by J. F. Lewkowicz, J. M. McPhetres and D. T. Reiter, Annapolis MD, PL-TR-96-2153, ADA313692.

Peterson, J. (1993), "Observations and Modeling of Seismic Background Noise," U.S.G.S. Open-File Report 93-322.

Sweeney, J. J. (1995), "Preliminary Maps of Crustal thickness and Regional Seismic Phases for the Middle East and North Africa," Lawrence Livermore National Laboratory Report UCRL-ID-122080.

Ringdal, F. (1976), "Maximum Likelihood Estimation of Seismic Magnitude," *Bull. Seism. Soc. Am.*, **66**(3), 789-802.

Vernon, F. R., R. J. Mellors, J. Berger, A. M. Al-Amri, and J. Zollweg, (1996), "Initial Results from the Deployment of Broadband Seismometers in the Saudi Arabian Shield," *Proceedings of the 18th Annual Seismic Research Symposium on Monitoring a Comprehensive Test Ban Treaty*, edited by J. F. Lewkowicz, J. M. McPhetres and D. T. Reiter, Annapolis MD, PL-TR-96-2153, ADA313692.

Von Seggern, D. and D. W. Rivers (1978), "Comments on the Use of Truncated Distribution Theory for Improved Magnitude Estimation," *Bull. Seism. Soc. Am.*, **68**(5), 1543-1546.

THOMAS AHRENS
SEISMOLOGICAL LABORATORY 252-21
CALIFORNIA INSTITUTE OF TECHNOLOGY
PASADENA, CA 91125

RALPH ALEWINE
NTPO
1901 N. MOORE STREET, SUITE 609
ARLINGTON, VA 22209

SHELTON ALEXANDER
PENNSYLVANIA STATE UNIVERSITY
DEPARTMENT OF GEOSCIENCES
537 DEIKE BUILDING
UNIVERSITY PARK, PA 16801

MUAWIA BARAZANGI
INSTITUTE FOR THE STUDY OF THE CONTINENTS
3126 SNEE HALL
CORNELL UNIVERSITY
ITHACA, NY 14853

RICHARD BARDZELL
ACIS
DCI/ACIS
WASHINGTON, DC 20505

T.G. BARKER
MAXWELL TECHNOLOGIES
P.O. BOX 23558
SAN DIEGO, CA 92123

DOUGLAS BAUMGARDT
ENSCO INC.
5400 PORT ROYAL ROAD
SPRINGFIELD, VA 22151

THERON J. BENNETT
MAXWELL TECHNOLOGIES
11800 SUNRISE VALLEY DRIVE SUITE 1212
RESTON, VA 22091

WILLIAM BENSON
NAS/COS
ROOM HA372
2001 WISCONSIN AVE. NW
WASHINGTON, DC 20007

JONATHAN BERGER
UNIVERSITY OF CA, SAN DIEGO
SCRIPPS INSTITUTION OF OCEANOGRAPHY IGPP, 0225
9500 GILMAN DRIVE
LA JOLLA, CA 92093-0225

ROBERT BLANDFORD
AFTAC
1300 N. 17TH STREET
SUITE 1450
ARLINGTON, VA 22209-2308

STEVEN BRATT
NTPO
1901 N. MOORE STREET, SUITE 609
ARLINGTON, VA 22209

RHETT BUTLER
IRIS
1200 NEW YORK AVE., NW
SUITE 800
WASHINGTON, DC 20005

LESLIE A. CASEY
DOE
1000 INDEPENDENCE AVE. SW
NN-20
WASHINGTON, DC 20585-0420

CATHERINE DE GROOT-HEDLIN
UNIVERSITY OF CALIFORNIA, SAN DIEGO
INSTITUTE OF GEOPHYSICS AND PLANETARY PHYSICS
8604 LA JOLLA SHORES DRIVE
SAN DIEGO, CA 92093

STANLEY DICKINSON
AFOSR
110 DUNCAN AVENUE, SUITE B115
BOLLING AFB
WASHINGTON, D.C. 20332-001

SEAN DORAN
ACIS
DCI/ACIS
WASHINGTON , DC 20505

DIANE I. DOSER
DEPARTMENT OF GEOLOGICAL SCIENCES
THE UNIVERSITY OF TEXAS AT EL PASO
EL PASO, TX 79968

RICHARD J. FANTEL
BUREAU OF MINES
DEPT OF INTERIOR, BLDG 20
DENVER FEDERAL CENTER
DENVER, CO 80225

JOHN FILSON
ACIS/TMG/NTT
ROOM 6T11 NHB
WASHINGTON, DC 20505

MARK D. FISK
MISSION RESEARCH CORPORATION
735 STATE STREET
P.O. DRAWER 719
SANTA BARBARA, CA 93102-0719

ROBERT GEIL
DOE
PALAIS DES NATIONS, RM D615
GENEVA 10, SWITZERLAND

LORI GRANT
MULTIMAX, INC.
311C FOREST AVE. SUITE 3
PACIFIC GROVE, CA 93950

HENRY GRAY
SMU STATISTICS DEPARTMENT
P.O. BOX 750302
DALLAS, TX 75275-0302

I. N. GUPTA
MULTIMAX, INC.
1441 MCCORMICK DRIVE
LARGO, MD 20774

DAVID HARKRIDER
PHILLIPS LABORATORY
EARTH SCIENCES DIVISION
29 RANDOLPH ROAD
HANSCOM AFB, MA 01731-3010

JAMES HAYES
NSF
4201 WILSON BLVD., ROOM 785
ARLINGTON, VA 22230

THOMAS HEARN
NEW MEXICO STATE UNIVERSITY
DEPARTMENT OF PHYSICS
LAS CRUCES, NM 88003

MICHAEL HEDLIN
UNIVERSITY OF CALIFORNIA, SAN DIEGO
SCRIPPS INSTITUTION OF OCEANOGRAPHY IGPP, 0225
9500 GILMAN DRIVE
LA JOLLA, CA 92093-0225

DONALD HELMBERGER
CALIFORNIA INSTITUTE OF TECHNOLOGY
DIVISION OF GEOLOGICAL & PLANETARY SCIENCES
SEISMOLOGICAL LABORATORY
PASADENA, CA 91125

EUGENE HERRIN
SOUTHERN METHODIST UNIVERSITY
DEPARTMENT OF GEOLOGICAL SCIENCES
DALLAS, TX 75275-0395

ROBERT HERRMANN
ST. LOUIS UNIVERSITY
DEPARTMENT OF EARTH & ATMOSPHERIC SCIENCES
3507 LACLEDE AVENUE
ST. LOUIS, MO 63103

VINDELL HSU
HQ/AFTAC/TTR
1030 S. HIGHWAY A1A
PATRICK AFB, FL 32925-3002

ANTHONY IANNACCHIONE
BUREAU OF MINES
COCHRANE MILL ROAD
PO BOX 18070
PITTSBURGH, PA 15236-9986

RONG-SONG JIH
PHILLIPS LABORATORY
EARTH SCIENCES DIVISION
29 RANDOLPH ROAD
HANSCOM AFB, MA 01731-3010

THOMAS JORDAN
MASSACHUSETTS INSTITUTE OF TECHNOLOGY
EARTH, ATMOSPHERIC & PLANETARY SCIENCES
77 MASSACHUSETTS AVENUE, 54-918
CAMBRIDGE, MA 02139

LAWRENCE LIVERMORE NATIONAL LABORATORY
ATTN: TECHNICAL STAFF (PLS ROUTE)
PO BOX 808, MS L-200
LIVERMORE, CA 94551

LAWRENCE LIVERMORE NATIONAL LABORATORY
ATTN: TECHNICAL STAFF (PLS ROUTE)
PO BOX 808, MS L-207
LIVERMORE, CA 94551

LAWRENCE LIVERMORE NATIONAL LABORATORY
ATTN: TECHNICAL STAFF (PLS ROUTE)
PO BOX 808, MS L-221
LIVERMORE, CA 94551

LAWRENCE LIVERMORE NATIONAL LABORATORY
ATTN: TECHNICAL STAFF (PLS ROUTE)
LLNL
PO BOX 808, MS L-175
LIVERMORE, CA 94551

LAWRENCE LIVERMORE NATIONAL LABORATORY
ATTN: TECHNICAL STAFF (PLS ROUTE)
PO BOX 808, MS L-208
LIVERMORE, CA 94551

LAWRENCE LIVERMORE NATIONAL LABORATORY
ATTN: TECHNICAL STAFF (PLS ROUTE)
PO BOX 808, MS L-202
LIVERMORE, CA 94551

LAWRENCE LIVERMORE NATIONAL LABORATORY
ATTN: TECHNICAL STAFF (PLS ROUTE)
PO BOX 808, MS L-195
LIVERMORE, CA 94551

LAWRENCE LIVERMORE NATIONAL LABORATORY
ATTN: TECHNICAL STAFF (PLS ROUTE)
PO BOX 808, MS L-205
LIVERMORE, CA 94551

THORNE LAY
UNIVERSITY OF CALIFORNIA, SANTA CRUZ
EARTH SCIENCES DEPARTMENT
EARTH & MARINE SCIENCE BUILDING
SANTA CRUZ, CA 95064

ANATOLI L. LEVSHIN
DEPARTMENT OF PHYSICS
UNIVERSITY OF COLORADO
CAMPUS BOX 390
BOULDER, CO 80309-0309

DONALD A. LINGER
DNA
6801 TELEGRAPH ROAD
ALEXANDRIA, VA 22310

LOS ALAMOS NATIONAL LABORATORY
ATTN: TECHNICAL STAFF (PLS ROUTE)
PO BOX 1663, MS F659
LOS ALAMOS, NM 87545

LOS ALAMOS NATIONAL LABORATORY
ATTN: TECHNICAL STAFF (PLS ROUTE)
PO BOX 1663, MS F665
LOS ALAMOS, NM 87545

LOS ALAMOS NATIONAL LABORATORY
ATTN: TECHNICAL STAFF (PLS ROUTE)
PO BOX 1663, MS D460
LOS ALAMOS, NM 87545

LOS ALAMOS NATIONAL LABORATORY
ATTN: TECHNICAL STAFF (PLS ROUTE)
PO BOX 1663, MS C335
LOS ALAMOS, NM 87545

GARY MCCARTOR
SOUTHERN METHODIST UNIVERSITY
DEPARTMENT OF PHYSICS
DALLAS, TX 75275-0395

KEITH MCLAUGHLIN
MAXWELL TECHNOLOGIES
P.O. BOX 23558
SAN DIEGO, CA 92123

BRIAN MITCHELL
DEPARTMENT OF EARTH & ATMOSPHERIC SCIENCES
ST. LOUIS UNIVERSITY
3507 LACLEDE AVENUE
ST. LOUIS, MO 63103

RICHARD MORROW
USACDA/IVI
320 21ST STREET, N.W.
WASHINGTON, DC 20451

JOHN MURPHY
MAXWELL TECHNOLOGIES
11800 SUNRISE VALLEY DRIVE SUITE 1212
RESTON, VA 22091

JAMES NI
NEW MEXICO STATE UNIVERSITY
DEPARTMENT OF PHYSICS
LAS CRUCES, NM 88003

JOHN ORCUTT
INSTITUTE OF GEOPHYSICS AND PLANETARY PHYSICS
UNIVERSITY OF CALIFORNIA, SAN DIEGO
LA JOLLA, CA 92093

PACIFIC NORTHWEST NATIONAL LABORATORY
ATTN: TECHNICAL STAFF (PLS ROUTE)
PO BOX 999, MS K6-48
RICHLAND, WA 99352

PACIFIC NORTHWEST NATIONAL LABORATORY
ATTN: TECHNICAL STAFF (PLS ROUTE)
PO BOX 999, MS K7-34
RICHLAND, WA 99352

PACIFIC NORTHWEST NATIONAL LABORATORY
ATTN: TECHNICAL STAFF (PLS ROUTE)
PO BOX 999, MS K6-40
RICHLAND, WA 99352

PACIFIC NORTHWEST NATIONAL LABORATORY
ATTN: TECHNICAL STAFF (PLS ROUTE)
PO BOX 999, MS K5-12
RICHLAND, WA 99352

KEITH PRIESTLEY
DEPARTMENT OF EARTH SCIENCES
UNIVERSITY OF CAMBRIDGE
MADINGLEY RISE, MADINGLEY ROAD
CAMBRIDGE, CB3 OEZ UK

PAUL RICHARDS
COLUMBIA UNIVERSITY
LAMONT-DOHERTY EARTH OBSERVATORY
PALISADES, NY 10964

CHANDAN SAIKIA
WOOODWARD-CLYDE FEDERAL SERVICES
566 EL DORADO ST., SUITE 100
PASADENA, CA 91101-2560

SANDIA NATIONAL LABORATORY
ATTN: TECHNICAL STAFF (PLS ROUTE)
DEPT. 5791
MS 0567, PO BOX 5800
ALBUQUERQUE, NM 87185-0567

SANDIA NATIONAL LABORATORY
ATTN: TECHNICAL STAFF (PLS ROUTE)
DEPT. 5704
MS 0655, PO BOX 5800
ALBUQUERQUE, NM 87185-0655

THOMAS SERENO JR.
SCIENCE APPLICATIONS INTERNATIONAL CORPORATION
10260 CAMPUS POINT DRIVE
SAN DIEGO, CA 92121

ROBERT SHUMWAY
410 MRAK HALL
DIVISION OF STATISTICS
UNIVERSITY OF CALIFORNIA
DAVIS, CA 95616-8671

DAVID SIMPSON
IRIS
1200 NEW YORK AVE., NW
SUITE 800
WASHINGTON, DC 20005

PACIFIC NORTHWEST NATIONAL LABORATORY
ATTN: TECHNICAL STAFF (PLS ROUTE)
PO BOX 999, MS K6-84
RICHLAND, WA 99352

FRANK PILOTTE
HQ/AFTAC/TT
1030 S. HIGHWAY A1A
PATRICK AFB, FL 32925-3002

JAY PULLI
RADIX SYSTEMS, INC.
6 TAFT COURT
ROCKVILLE, MD 20850

DAVID RUSSELL
HQ AFTAC/TTR
1030 SOUTH HIGHWAY A1A
PATRICK AFB, FL 32925-3002

SANDIA NATIONAL LABORATORY
ATTN: TECHNICAL STAFF (PLS ROUTE)
DEPT. 5704
MS 0979, PO BOX 5800
ALBUQUERQUE, NM 87185-0979

SANDIA NATIONAL LABORATORY
ATTN: TECHNICAL STAFF (PLS ROUTE)
DEPT. 9311
MS 1159, PO BOX 5800
ALBUQUERQUE, NM 87185-1159

SANDIA NATIONAL LABORATORY
ATTN: TECHNICAL STAFF (PLS ROUTE)
DEPT. 5736
MS 0655, PO BOX 5800
ALBUQUERQUE, NM 87185-0655

AVI SHAPIRA
SEISMOLOGY DIVISION
THE INSTITUTE FOR PETROLEUM RESEARCH AND GEOPHYSICS
P.O.B. 2286, NOLON 58122 ISRAEL

MATTHEW SIBOL
ENSCO, INC.
445 PINEDA COURT
MELBOURNE, FL 32940

JEFFRY STEVENS
MAXWELL TECHNOLOGIES
P.O. BOX 23558
SAN DIEGO, CA 92123

BRIAN SULLIVAN
BOSTON COLLEGE
INSITUTE FOR SPACE RESEARCH
140 COMMONWEALTH AVENUE
CHESTNUT HILL, MA 02167

DAVID THOMAS
ISEE
29100 AURORA ROAD
CLEVELAND, OH 44139

NAFI TOKSOZ
EARTH RESOURCES LABORATORY, M.I.T.
42 CARLTON STREET, E34-440
CAMBRIDGE, MA 02142

LAWRENCE TURNBULL
ACIS
DCI/ACIS
WASHINGTON, DC 20505

GREG VAN DER VINK
IRIS
1200 NEW YORK AVE., NW
SUITE 800
WASHINGTON, DC 20005

FRANK VERNON
UNIVERSITY OF CALIFORNIA, SAN DIEGO
SCRIPPS INSTITUTION OF OCEANOGRAPHY IGPP, 0225
9500 GILMAN DRIVE
LA JOLLA, CA 92093-0225

TERRY WALLACE
UNIVERSITY OF ARIZONA
DEPARTMENT OF GEOSCIENCES
BUILDING #77
TUCSON, AZ 85721

DANIEL WEILL
NSF
EAR-785
4201 WILSON BLVD., ROOM 785
ARLINGTON, VA 22230

JAMES WHITCOMB
NSF
NSF/ISC OPERATIONS/EAR-785
4201 WILSON BLVD., ROOM785
ARLINGTON, VA 22230

RU SHAN WU
UNIVERSITY OF CALIFORNIA SANTA CRUZ
EARTH SCIENCES DEPT.
1156 HIGH STREET
SANTA CRUZ, CA 95064

JIAKANG XIE
COLUMBIA UNIVERSITY
LAMONT DOHERTY EARTH OBSERVATORY
ROUTE 9W
PALISADES, NY 10964

JAMES E. ZOLLWEG
BOISE STATE UNIVERSITY
GEOSCIENCES DEPT.
1910 UNIVERSITY DRIVE
BOISE, ID 83725

OFFICE OF THE SECRETARY OF DEFENSE
DDR&E
WASHINGTON, DC 20330

DEFENSE TECHNICAL INFORMATION CENTER
8725 JOHN J. KINGMAN ROAD
FT BELVOIR, VA 22060-6218 (2 COPIES)

TACTEC
BATTELLE MEMORIAL INSTITUTE
505 KING AVENUE
COLUMBUS, OH 43201 (FINAL REPORT)

PHILLIPS LABORATORY
ATTN: XPG
29 RANDOLPH ROAD
HANSCOM AFB, MA 01731-3010

PHILLIPS LABORATORY
ATTN: GPE
29 RANDOLPH ROAD
HANSCOM AFB, MA 01731-3010

PHILLIPS LABORATORY
ATTN: TSML
5 WRIGHT STREET
HANSCOM AFB, MA 01731-3004

PHILLIPS LABORATORY
ATTN: PL/SUL
3550 ABERDEEN AVE SE
KIRTLAND, NM 87117-5776 (2 COPIES)